

pubs.acs.org/Macromolecules Article

Predicting χ from Concentration Response to Spatially Varying **Potentials**

Puja Agarwala, Enrique D. Gomez, and Scott T. Milner*



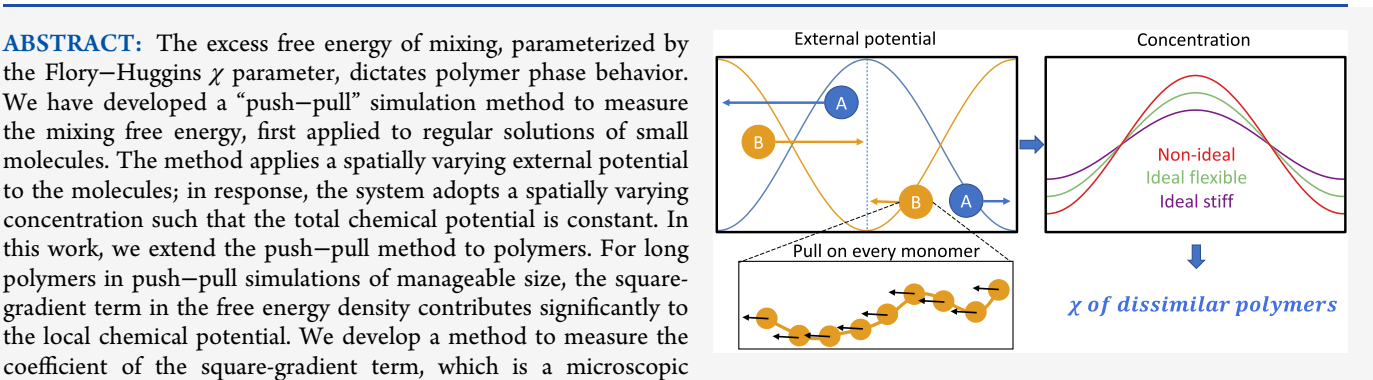
Cite This: Macromolecules 2023, 56, 6859-6869



ACCESS I

Metrics & More

ABSTRACT: The excess free energy of mixing, parameterized by the Flory-Huggins χ parameter, dictates polymer phase behavior. We have developed a "push-pull" simulation method to measure the mixing free energy, first applied to regular solutions of small molecules. The method applies a spatially varying external potential to the molecules; in response, the system adopts a spatially varying concentration such that the total chemical potential is constant. In this work, we extend the push-pull method to polymers. For long polymers in push-pull simulations of manageable size, the squaregradient term in the free energy density contributes significantly to the local chemical potential. We develop a method to measure the



Article Recommendations

length of order of the persistence length. We then validate the push-pull method by applying it to both bead-spring and chemically realistic polymer blends and comparing to χ values from our previously developed "morphing" technique. The new push-pull approach has two important advantages: (1) only one simulation is required, and (2) the chains need not be structurally similar, which enables prediction of χ for polymer blends with any chemical structure.

INTRODUCTION

Polymer blends are widely used to achieve desirable properties unobtainable in a pure material. Depending on the application, either miscible or immiscible blends are employed. In the commercial product family NORYL, which are polystyrene/ polyphenylene oxide miscible blends, mechanical properties such as softness vary smoothly with composition. In rubbertoughened plastics, brittle glassy polymers are toughened by a nanoscale dispersion of rubber domains, which impede crack propagation. Another emerging application of polymer blends is in organic photovoltaic cells, where an immiscible blend of donor polymers and small-molecule acceptors yields a bulk heterojunction material, filled with donor-acceptor interfaces at which excitons can dissociate.³⁻⁶

Entropy of mixing drives miscibility, but long polymer molecules gain little entropy per monomer on mixing, so small net repulsive interactions between monomers can overcome the entropy and lead to demixing. As a consequence, most blends of long polymers are immiscible, even when their constituent monomers are quite similar in structure. The net repulsive interaction between unlike monomers is represented phenomenologically by the Flory–Huggins χ parameter.^{8–10} For an ideal mixture, in which monomers are in every way identical except for labeling, χ equals zero. The Flory-Huggins theory subsumes the effects of all local properties such as composition, monomer architecture, and conformations that contribute to the local mixing free energy into a single

Experimentally, the χ parameter can be obtained in a variety of ways. 11 For binary blends of linear chains, χ can be determined from small-angle scattering from composition fluctuations in the miscible region, from analysis of the phase boundary, or from the width of the interface between phases in an immiscible blend. For diblock copolymers, χ can be determined likewise from small-angle scattering from composition fluctuations in the miscible region, or from the location of the order-disorder transition as a function of chain length.

All of these approaches rely on a comparison between experimental results and a theory of fluctuations and phase behavior. Simple mean-field theories treat fluctuations in harmonic approximation and are not accurate in the critical region. When χ is small as is commonly the case, miscible blends of long chains can be studied, and mean-field theory works tolerably well outside a narrow critical region. For symmetric diblock copolymers, the second-order transition

Received: April 24, 2023 Revised: August 2, 2023 Published: August 28, 2023





© 2023 American Chemical Society

predicted by mean-field theory is driven first order by long-wavelength fluctuations, for which a proper description requires more sophisticated theory.¹²

Morse and co-workers have developed a sophisticated approach to measuring χ in simulations, in which they simulate a symmetric diblock copolymer melt, determine the structure factor S(q), and infer χ by comparing S(q) to predictions of their renormalized one-loop theory. They use symmetric diblocks, in part because the critical χ is higher than for binary linear blends, so larger χ values can be accessed within the disordered phase for a given chain length.

While this approach has been successful, 15,16 the analysis is somewhat involved, and at present restricted to symmetric systems (conformationally symmetric blocks with equal lengths). This precludes its application to systems that break these symmetries, including blends of unequal volume fractions (necessary to treat compositional dependence of χ), as well as chains with different monomer volumes or chain stiffness (which are ubiquitous in chemically realistic polymers).

Multiple simulation techniques have been developed to measure the mixing free energy and the Flory–Huggins parameter χ . Gibbs ensemble Monte Carlo (GEMC) simulation measures the concentration of coexisting phases, which requires swapping of molecules from one phase to another to equalize the chemical potential. ^{17,18} For polymers, the acceptance rate is very low and difficult to measure. Chen et al. improved the GEMC method for polymers by enhancing the low acceptance rate calculation using impurity molecule and identity switch moves. ¹⁹ But for complex polymer architectures, acceptance rate calculations are difficult to implement. ²⁰

Kirkwood–Buff theory has been used to compute χ parameters, via a thermodynamic relation that connects excess free energies to integrals of pair correlation functions. However, the practical application of Kirkwood–Buff theory requires long simulations of large systems, to achieve pair correlation functions of sufficient accuracy and extent that the integrals converge well.

Our group has developed several methods to evaluate χ . Kozuch et al. developed a "morphing" technique, ²³ which computes the work to transform one kind of polymer (A) into another (B). By comparing the work to transform A into B in an A–B mixture to the work to transform pure A into pure B, the mixing free energy can be determined. The morphing method showed that bead-spring polymers with identical interactions between beads nonetheless have a repulsive χ if one chain species is stiffer than another, which increases with stiffness mismatch.

Zhang et al. applied the morphing method to compute χ between bead-spring polymers of identical stiffness, but with different Lennard-Jones interactions. ²⁴ Shetty et al. extended the morphing method to blends of chemically realistic polymers, such as polyethylene/polyethylene oxide blends and polyisoprene/saturated polyisoprene blends, by computing the work to transform the atoms of one chain into those of another. ²⁵ Because the morphing method requires one polymer to morph into another, its application is limited to polymers with similar architecture.

To extend morphing methods to structurally dissimilar polymers, Shetty et al. developed the "mutual ghosting" method.²⁶ This method computes the thermodynamic work to weaken the interaction between two components until they phase-separate. The interfacial tension between the two

immiscible phases is then measured by standard techniques. The mixing free energy is then the thermodynamic work minus the interfacial free energy. This method gives results in good agreement with morphing calculations on bead-spring chains, as well as small molecules and polymers of similar structure, for which morphing calculations can be performed. However, mutual ghosting fails for mixtures of stiff polymers because the interface between the demixed polymers leads to molecular ordering. ^{27,28}

A more recent and robust method developed in our group is the "push—pull" technique by Mkandawire et al., ²⁹ first applied to benzene—pyridine mixtures. In this method, a spatially varying external potential applied to every molecule in a mixture induces a varying concentration. The same external potential applied to a repulsive nonideal mixture induces a larger concentration variation than for an ideal mixture because repulsions between molecules amplify the effect; a system nearer to demixing has a larger susceptibility to potentials that induce a concentration variation. By analyzing the resulting concentration profile and fitting to standard free energy models, χ parameters can be measured.

Compared to previous approaches, the push—pull method has several advantages. It requires only one simulation in the presence of an external potential, while the morphing and mutual ghosting methods require an entire sequence of simulations, along which some thermodynamic interaction parameters are progressively varied. Like mutual ghosting, the push—pull method does not require structural similarity of the molecules in the mixture. But unlike mutual ghosting, the push—pull method does not induce complete demixing, and so avoids the formation of an interface that may cause molecular ordering. Finally, the push—pull method appears to be less sensitive to finite-size effects, compared to the Kirkwood—Buff method.

In this work, we extend the push—pull method to polymers. For polymers, we find that square-gradient terms in the free energy density contribute significantly to the local chemical potential, for the size of system we are conveniently able to simulate, and the magnitude of χ parameters we are seeking. Thus, we develop a method to measure the square-gradient coefficient, by applying external potentials to various ideal mixtures, for which the square-gradient term reveals itself as a correction to simple ideal solution theory. We expect the square-gradient coefficient should be a microscopic length, of order to the persistence length of the chains. We explore this dependence by measuring the square-gradient coefficient for bead-spring polymers with varying stiffness.

We validate the push–pull method by measuring χ for various polymer mixtures, including both bead-spring and chemically realistic chains, for which we have obtained χ previously with morphing and mutual ghosting. The systems we investigate here are:

- flexible bead-spring polymers with different Lennard-Jones interactions;
- 2. bead-spring polymers with identical Lennard-Jones interactions but different stiffness;²³ and
- 3. mixtures of oligomeric polyethylene (PE) and polyethylene oxide (PEO), ²⁵ for which experimental χ values are available. ³⁰

In all cases, results from the push-pull method agree well with previous simulation and experimental results, suggesting that

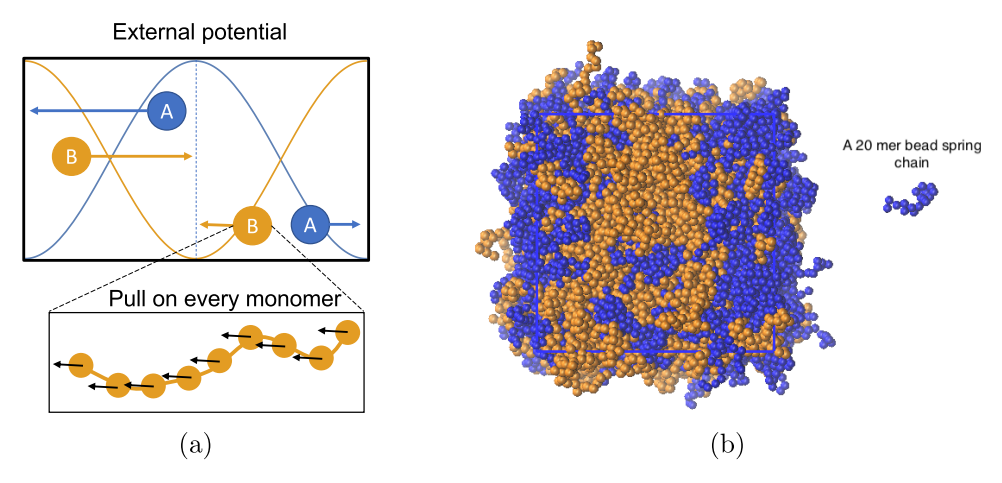


Figure 1. (a) Schematic of external potential pushing polymer A to the boundary and pulling B to the center. (b) Induced concentration gradient in polymer A (blue) and B (orange); right: single-chain configuration shown for size comparison.

the push–pull method will be widely useful in determining polymer χ parameters from simulation.

PUSH—PULL METHOD

In the push–pull method, ²⁹ equal and opposite external potentials are applied to every molecule of species A and B in a binary A-B blend. For polymers, we apply the external potential to every monomer (Figure 1a). In the original paper, harmonic potentials were used; here, we maintain smooth behavior at the periodic boundary by using a cosine potential

$$U(z) = k\cos(2\pi z/L) \tag{1}$$

where L is the simulation box length. A positive k pulls a molecule toward the middle, while a negative k pushes a molecule toward the boundary, inducing a concentration gradient as shown in Figure 1b. We choose k large enough that the concentration varies over a substantial range, but not so large that the system separates into pure phases.

In our investigations of bead-spring polymers and their blends, we study three different kinds of chains: (1) flexible bead-spring chains ("base"), (2) flexible bead-spring chains with weakened attractive interactions ("weak"), and (3) stiffened bead-spring chains ("stiff"). To apply the push—pull method to chemically realistic polymer blends, we study a mixture of polyethylene (PE) and polyethylene oxide (PEO).

The bead-spring chains are similar to those studied by Kozuch et al. 23 and Zhang et al. 24 Each chain is 20 beads long. Beads interact with Lennard-Jones (LJ) interactions $V_{LJ}(r)=4\epsilon\left((\frac{\sigma}{r})^{12}-\left(\frac{\sigma}{r}\right)^6\right)$, with σ equal to 0.2 nm for all beads. The LJ energy ϵ equals kT for the "base" and "stiff" chains, and is reduced to 0.88 kT for the "weak" chains. For all chains, bonded beads interact with a stiff harmonic spring potential $V_b=\frac{k_b}{2}(b-b_0)^2$, with a constant k_b equal to $400~kT/b_0^2$ and a bond length b_0 equal to $2^{1/6}\sigma$ (i.e., the minimum in the LJ potential). The cutoff distance for LJ interactions is taken as twice the LJ minimum, i.e., $2b_0$. The "base" and "weak" polymers have no angular spring potential $V_\theta=\frac{k_0}{2}(\theta-\theta_0)^2$, while the "stiff" polymer has angular springs

acting on the bond angles, with a spring constant k_{θ} of 2.5 kT.

All bead-spring simulations are performed at a temperature of 300K, maintained by a velocity rescaling thermostat. Equilibrations are performed with a pressure of $0.1~kT/\sigma^3$, maintained by a Berendsen barostat. Push—pull simulations are performed at constant volume, with the external potential applied to every bead. The bead-spring simulations contain 600 chains (12000 beads) unless explicitly stated otherwise. With a 2 fs timestep, equilibration simulations of 600 chains run at 520 ns/day on 16 cores without GPU.

Push-pull simulations are substantially slower, presumably because of the computational overhead in imposing potentials as currently implemented in Gromacs. To investigate this overhead, we performed a series of simulations on a system of 24000 beads, with fixed hardware (32 cores, 2 GPUs) with an increasing number of external potentials imposed on individual beads. We find that the total computational time scales linearly with the number of imposed potentials as expected, but with a surprisingly large slope: each potential term takes as much time to evaluate as the force on 24 beads. This must reflect an inefficiency in how Gromacs implements pull potentials; possibly, the code "reinterprets" the pull commands at each timestep. In an efficient implementation, imposing a cosine potential on a particle should be computationally cheaper than computing the total force on that particle; the present inefficient implementation in Gromacs should not be regarded as a fundamental limitation to our method.

The PE-PEO mixture simulated here is the same as studied by Shetty et al.²⁵ The PE and PEO chains consist of 15 and 10 monomers (so that a PE chain can be morphed into a PEO chain by converting every third CH₂ into an ether O). For the PE-PEO system, we perform united atom (UA) simulations using TraPPE potential parameters.³¹ To determine the appropriate simulation volume for the mixture, we simulate pure PE and pure PEO system at 500 K and 1 bar, and assume zero volume change on mixing. We find 10.58 and 8.36 monomers per 0.1 nm³ volume for PE and PEO, respectively.

For PE-PEO, our system consists of 200 chains each and totals 12000 atoms (see Figure 2). For the push-pull simulations, we equilibrate at 500 K and 1 bar followed by push-pull simulations at constant volume. To economize on the overhead of imposing thousands of external potentials, because PE and PEO chains are somewhat stiff, we pull on groups of three successive atoms along each chain, for a total of 4000 external potential terms, with 2 fs timestep equilibration

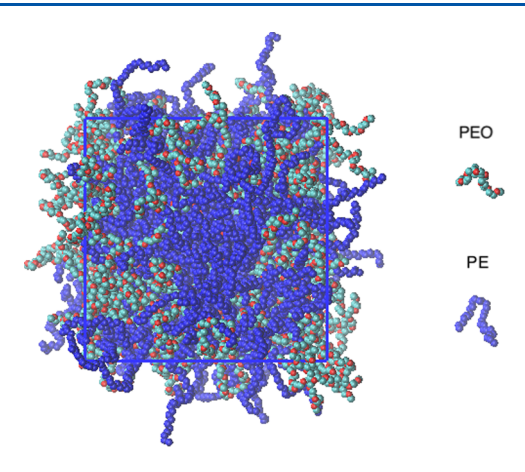


Figure 2. Simulation snapshot for PE-PEO mixture with applied cosine potential; single PE and PEO configurations shown for size comparison.

simulations run at 215 ns/day on 16 cores with one GPU and push-pull simulations run at 110 ns/day on 32 cores with 4 GPUs.

MIXING FREE ENERGY

To extract χ parameters from push–pull simulations, Mkandawire et al. fitted their results to predictions of a regular-solution free energy under an applied external potential, written as²⁹

$$\beta \Delta G = \sum_{i} \phi_{i} \log \phi_{i} + (1/2) \sum_{ij} \chi_{ij} \phi_{i} \phi_{j} + \beta \sum_{i} \phi_{i} U_{i}$$
(2)

Here, ϕ_i is the mol fraction of component i, U_i is the external potential applied to component i, and χ_{ij} is the interaction parameter between species i and j. The free energy is the sum

of ideal mixing (first term), interaction between species (second term), and external potentials (third term).

At equilibrium, the free energy is minimized with respect to the mole fractions ϕ_i . For a binary mixture, the resulting relation between the external potential and concentration takes the form

$$\beta U(\phi) = -\log\left(\frac{\phi}{1-\phi}\right) - \chi(1-2\phi) \tag{3}$$

where $U(\phi)$ denotes the difference $U_1(\phi) - U_2(\phi)$, ϕ is the mole fraction of species 1, and χ equals $\chi_{AB} - (1/2)(\chi_{AA} + \chi_{BB})$. For an ideal mixture, χ vanishes.

To find out whether this simple description works for an ideal polymer mixture, we perform push—pull simulations on an ideal mixture of two components "base1" and "base2", both with the properties of the "base" chains, differing only in their labels. We applied equal and opposite external potentials to every bead, with $k_{\rm base1} = -k_{\rm base2} = \frac{0.75\,kT}{2\,N}$ (see Figure 3a). We applied this same protocol to an ideal mixture of two components "stiff1" and "stiff2", both with the properties of the "stiff" chains.

Figure 3b presents the resulting concentration profiles; Figure 3c shows the simulated and predicted behavior (from eq 3) of the external potential versus concentration. The simulated ideal mixtures require a larger external potential to induce a given concentration shift than the ideal solution theory predicts. This discrepancy between simulation results and ideal solution theory is evidently larger for stiff chains than for flexible chains. Certainly, eq 3 does not describe our push—pull simulation results for ideal polymer mixtures.

MEASURING SQUARE-GRADIENT TERMS

Ideal solution theory without a square-gradient contribution does not agree with our push-pull simulation results for ideal

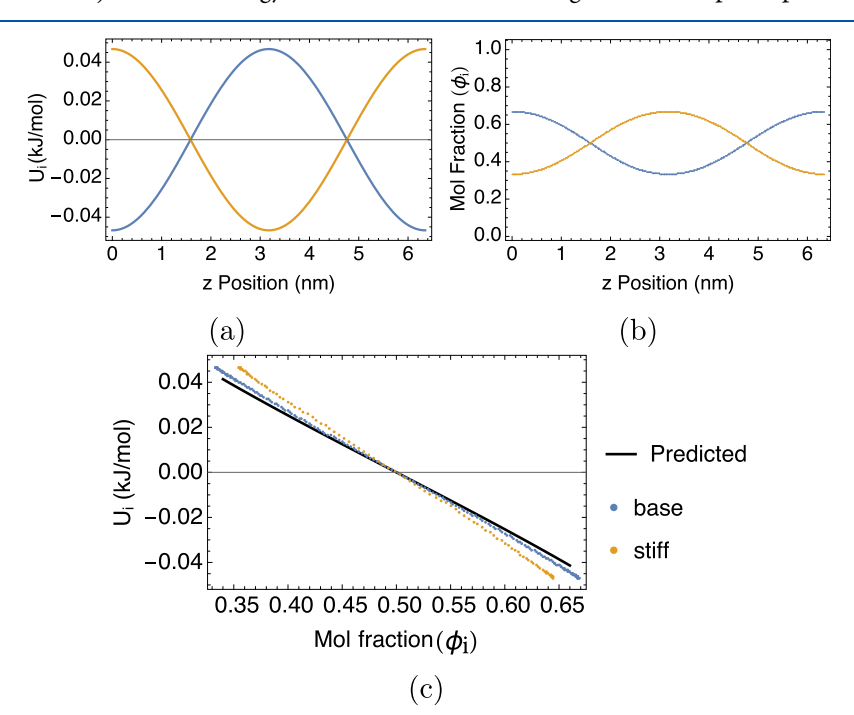


Figure 3. (a) External potential and (b) induced mol fraction versus z, for ideal flexible chain mixture of base1 (orange) and base2 (blue). (c) Predicted external potential (black) from eq 3 versus push-pull results for ideal mixtures of base (blue) and stiff (orange) chains.

chains, because for our polymer simulations, the system is small enough that square-gradient terms are not negligible compared to the ideal chain entropy of mixing. Thus, we write the free energy including square-gradient terms, as

$$\beta G = A \int \left(\sum \frac{\phi_i}{N_i} \log \phi_i + (1/2) \sum \chi_{ij} \phi_i \phi_j + \sum \phi_i \beta U_i(z) + \frac{a_i^2}{2} (\nabla \phi_i)^2 \right) dz$$
(4)

Here, A is the transverse area of the system; ϕ_i , N_i , and a_i are the volume fraction, number of monomers, and square-gradient term coefficient of polymer i, respectively; and U_i is the external potential applied on polymer i.

In principle, the full ideal single-chain structure function $F^{-1}(q)$ (i.e., the reciprocal of the Debye function) should appear in the effective Hamiltonian, not just a square-gradient term. However, our systems are large enough so that q^2Rg^2 is small (0.15 for bead-spring chains, about 0.5 for PE and PEO), as is visually evident in Figures 1b and 2. Thus, $F^{-1}(q)$ is well approximated by expanding to $O(q^2)$, with corrections at the 1% level. More generally, the Debye function itself is an approximation for real chains (it assumes ideal Gaussian chains at all scales). We prefer not to rely on its detailed validity, so we ensure our system is large enough that a square-gradient approximation is justified.

For a binary mixture of species *A* and *B*, minimizing the free energy with respect to the concentration field results in

$$\beta U = -\left(\frac{\log(\phi)}{N_A} - \frac{\log(1-\phi)}{N_B}\right) - \chi(1-2\phi) + (a_A^2 + a_B^2)\nabla^2\phi$$
(5)

We can compare the contributions of square-gradient terms and chain entropy of mixing by a scaling argument. The square-gradient contribution is of order $a^2\nabla^2\phi$, while the entropy of mixing contribution is of order (1/N). Since the gradient $\nabla\phi$ is of order 1/L, where L is the simulation box dimension, these terms are comparable when Na^2 is comparable to L^2 . Polymer simulations of manageable size typically have box dimensions not too much larger than the chain end-to-end distance, so square-gradient terms are never negligibly small.

For an ideal polymer blend with $\chi=0$, the square-gradient terms must make up the difference between the push—pull simulation results for $\beta U(\phi)$ and the ideal solution prediction without gradient terms (Figure 3c). We can therefore use ideal solution results to measure the square-gradient coefficient a. We can validate this approach to measuring square-gradient coefficients by varying the box dimension, and verifying that we get the same value of a for different box sizes. By measuring a for flexible and stiff bead-spring chains, we can show that a is related to the persistence length of the chains.

For a cosine external potential of moderate amplitude, the concentration variation $\Delta\phi(z)$ will likewise be cosinusoidal, proportional to $\cos(2\pi z/L)$. Hence, $\nabla^2\phi$ will equal $-(2\pi/L)^2\phi$ so that

$$\beta U(\phi) = -\frac{1}{N} \log \left(\frac{\phi}{1 - \phi} \right) - 2a^2 \left(\frac{2\pi}{L} \right)^2 (\phi - \overline{\phi})$$
 (6)

where $\overline{\phi}$ is the average concentration. Hence, the square-gradient correction to the external potential versus concen-

tration $\beta U(\phi)$ will be linear in ϕ , with a slope $-2a^2(2\pi/L)^2$ that varies with the box dimension L as $1/L^2$. The linear dependence on ϕ is evident in Figure 3c. To check the dependence on L, we perform push-pull simulations with different box sizes.

We simulate two ideal mixtures of base polymers: a larger system of 1200 chains and a smaller system of 600 chains. The equilibrated box lengths for the large and small systems are 6.35 and 5.04 nm, respectively. For both systems, we divide the polymers into base1 and base2 species containing an equal number of chains and apply the push—pull method (Figure 1a) with $k_{\text{base1}} = -k_{\text{base2}} = 0.047$. We obtain induced concentration profiles by averaging over simulations of 1000 ns duration.

We subtract the ideal-mixing contribution from the measured $\beta U(\phi)$ to obtain the square-gradient term (SGT), shown in Figure 4. For both the large and small systems, the

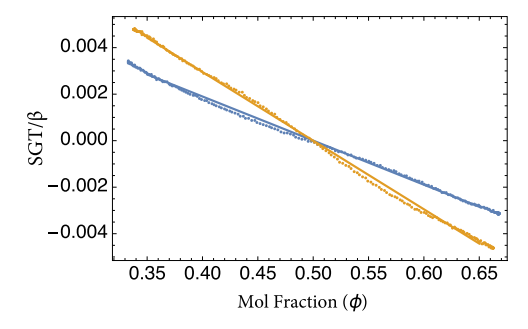


Figure 4. Square-gradient term (SGT) in $\beta U(\phi)$ for an ideal mixture of flexible bead-spring chains, for large (orange) and small (blue) simulation boxes.

square-gradient contribution is linear in ϕ as expected. Furthermore, the slopes scale as $1/L^2$; the slope for the small system (orange) is 1.59 times that of the large system (blue), which equals $(L_2/L_1)^2 = 2^{2/3}$ as expected. Equating the slope of the square-gradient contribution to $2a^2(2\pi/L)^2$, we find a = 0.117 nm for our flexible bead-spring chains.

■ MEASURING A IN MIXTURES

To apply the push—pull method to nonideal mixtures, we need square-gradient coefficients for mixtures as well as pure components. One approach is to measure a_A and a_B for the A and B components separately, and then to assume the coefficients for each species are the same in the mixture as in the pure phases.

Alternatively, we can measure the square-gradient terms for both components in a mixture directly, by dividing the A and B chains into two components differing only in their labels (denoted A1 and A2 and B1 and B2), then applying the same cosine potential to A1 and B1, and the opposite potential to A2 and B2 (see Figure 5). The physically relevant concentrations of A and B remain spatially uniform when potentials are applied to the "1" and "2" chains. Effectively, we are performing simultaneous push—pull simulations on an ideal A1—A2 mixture and an ideal B1—B2 mixture within the overall A-B system. With these "split-component" push—pull simulations, we can measure the square-gradient coefficients a_A and a_B directly in the mixture, which allows us to check whether the coefficients change when pure components are mixed.

We apply this method to our three blends of interest: base—weak and base—stiff bead-spring chains, and chemically realistic PE—PEO oligomers. In all cases, we equilibrate the

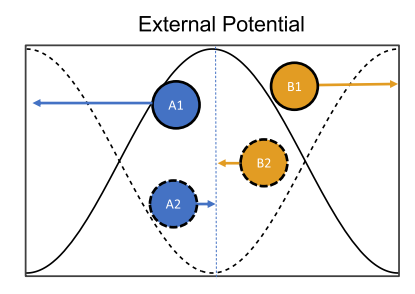


Figure 5. Schematic of external potential applied to A chains (blue) subdivided into A1 (solid) and A2 (dashed) and B chains (orange) subdivided into B1 (solid) and B2 (dashed), for measuring square-gradient term in mixtures.

systems for 100 ns as previously described and then measure the average concentration profiles over a 500 ns simulation. Resulting concentration profiles for split-component push—pull simulations of all three blends are shown in Figure 6a—c. Figure 6d—f displays the same results plotted as applied external potential $U(\phi)$ as a function of induced concentration ϕ for each component.

For the base—weak polymer mixture, the concentration profiles for base and weak chains are the same (see Figure 6a). Because the external potentials applied to the base and weak chains were the same, evidently the square-gradient coefficient is the same for base and weak chains (see Table 1 for a values, fitted from results in Figure 6d). Base and weak chains are equally flexible, differing only in the strength of their nonbonded interactions, suggesting that the value of a depends mainly on persistence length.

To learn how a depends on persistence length, we examine results for the base—stiff polymer mixture (Figure 6b). Qualitatively, the stiff polymer exhibits a weaker concentration variation than the base polymer, consistent with a stronger square-gradient term that penalizes concentration gradients.

Table 1. Square-Gradient Coefficients a Measured by Split-Component Push—Pull Method

system	$a_{\rm A}$ (nm)	$a_{\rm B}~({\rm nm})$
base-weak	0.1163	0.1175
base-stiff	0.1254	0.2095
PE-PEO	0.2951	0.2696

The fitted values of a for base and stiff polymers in the mixture are consistent with this observation (see Table 1); we find $a_{\rm base} = 0.1254$, versus $a_{\rm stiff} = 0.2095$. The base and stiff chains have identical nonbonded interactions, but the stiff chain has a persistence 4 times that of the base chain (directly measured from the decay of the tangent autocorrelation function).

The value of a_{base} in the mixture is slightly larger than in a pure base melt (a = 0.125 versus a = 0.117), presumably because blending with the stiff polymer increases the persistence length of the base polymer, which is 3% larger in the base—stiff mixture than in the pure base melt. Thus, the square-gradient coefficient for components in a mixture may not be identical to the corresponding pure phase values, although the effect in the present case is modest.

We use the same approach to evaluate the square-gradient coefficients for PE and PEO oligomers in an equimolar blend. In this case, we apply a cosine potential with amplitude k=0.208 to successive groups of three atoms along each chain. Figure 6c shows the induced concentration profiles, and Figure 6f shows the corresponding plot of external potential $U(\phi)$ versus concentration. Table 1 reports the fitted values of $a_{\rm PE}$ and $a_{\rm PEO}$; note that PE, with a persistence length of 7 Å, has a slightly larger coefficient than PEO, with a persistence length of 5.06 Å.

\blacksquare MEASURING χ

With values for the square-gradient coefficients in hand, we can perform and analyze push—pull simulations for base—weak,

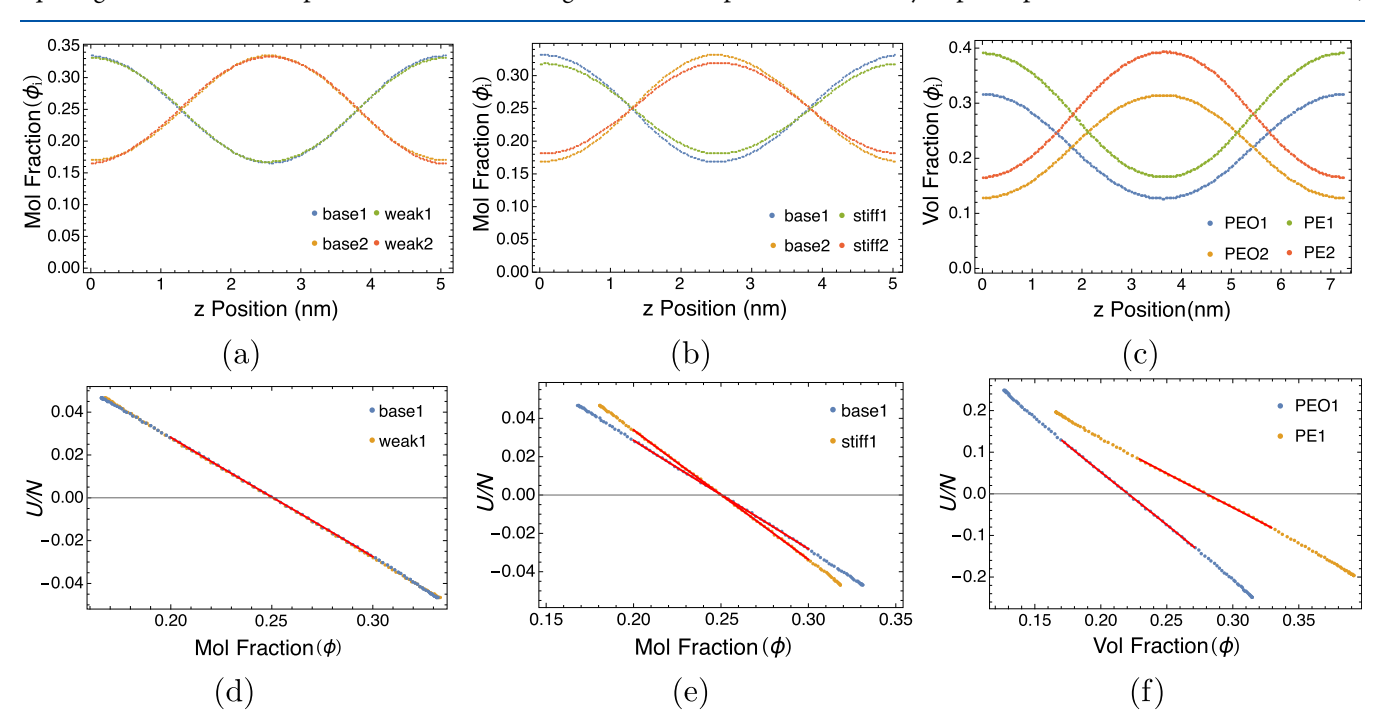


Figure 6. Induced concentration variations versus z for "split-component" push-pull simulations of base-weak (a), base-stiff (b), and PE-PEO (c) mixtures; (d-f) plots of these same results as $U(\phi)$, with fits (red lines) to determine square-gradient terms.

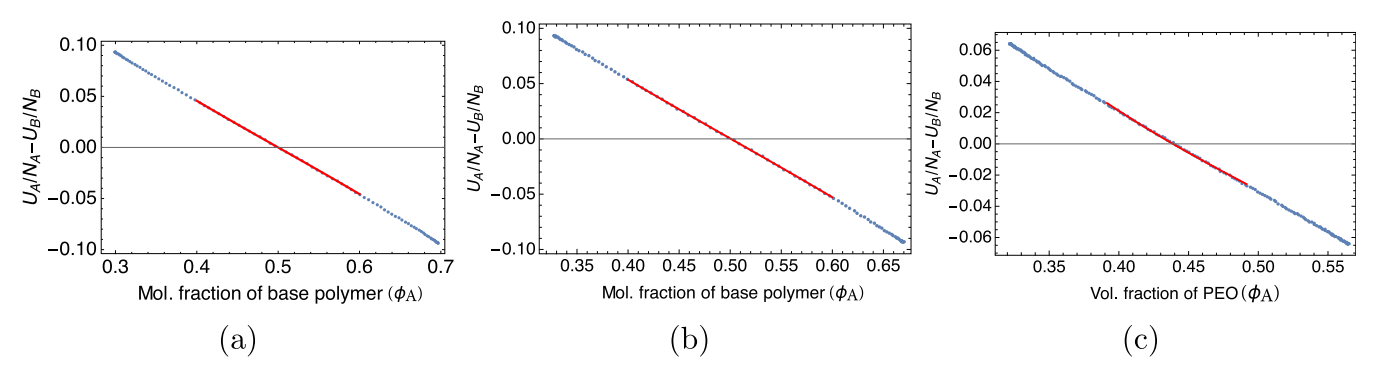


Figure 7. External potential $U(\phi)$ versus concentration ϕ from simulation (blue) and fit (red) to eq 5 for (a) base—weak, (b) base—stiff, and (c) PE-PEO polymers.

base—stiff, and PE—PEO polymer blends to measure the Flory—Huggins χ parameters and compare our results to values obtained previously using morphing simulations. For each system, we pull one species toward the center and push the other toward the boundaries, as shown in Figure 1a.

We measure the resulting concentration profiles $\phi(z)$; Figure 7 presents the results for all three blends plotted as external potential $U(\phi)$ versus ϕ . We focus on the central portion of the concentration dependence, to obtain the χ parameter relevant to small excursions of the concentration from the average value.

For the bead-spring polymer blends, we report χ per bead. For the PE-PEO blend, we follow experimental conventions and report χ per volume V_0 , defined as 0.1 nm³. (In terms of V_0 , the displaced volume per oligomer is 10.58 V_0 for PE and 8.36 V_0 for PEO.) Table 2 reports the results for χ .

Table 2. Comparison of χ Estimated from Push–Pull and Morphing Simulations.^a

system	push-pull	morphing	experiment
base-weak	0.023	0.020	N/A
base-stiff	0.024	0.022	N/A
PE-PEO	0.218	0.209	0.143

^aFor bead-spring chains, χ per bead; for PE-PEO, χ per 0.1 nm³.

We compare our push–pull results for χ of base–weak blends to results obtained using morphing. A very similar system was studied using morphing by Zhang et al.;²⁴ however, our potential parameters for the base and weak chains are slightly different, so we repeat the morphing simulation using the same method with 40 bead long polymer. In the morphing

method, we perform two series of simulations in which potential parameters are systematically varied to transform one type of chain into another. In the first series, we start from a pure base melt and morph half the base chains into weak chains; in the second series, we transform all of the base chains into weak chains. From the difference in thermodynamic work done to transform the mixed versus the pure phase, we can infer the excess mixing free energy, and hence χ .

To transform base into weak chains, we change the Lennard-Jones ϵ parameter from kT to 0.88 kT, defining λ such that $\epsilon(\lambda) = \lambda$ kT. The free energy integrand $\partial F/\partial \lambda$ equals simulation average $\langle \partial E/\partial \lambda \rangle$; the integrand varies smoothly with λ (see Figure 8a). Using morphing, we find a base—weak χ of 0.02 per bead, in good agreement with our push—pull result of $\chi=0.023$.

We compare our push–pull results for χ of base–stiff polymer blends to morphing simulations of Kozuch et al., ²³ who investigated blends bead-spring polymers with varying stiffness, with angular spring constant k_{θ} ranging from 0 to 3 kT. In particular, they report χ for blends of flexible bead-spring chains with $k_{\theta}=0$ with chains having $k_{\theta}=2.4$ kT, and also with chains having $k_{\theta}=2.6$ kT. We interpolate these results to obtain $\chi=0.022$ per bead corresponding to our base–stiff polymer mixture (stiff chains with $k_{\theta}=2.5$ kT), in good agreement with our push–pull result of $\chi=0.024$.

For the PE–PEO polymer blend, previous work using morphing simulations²⁵ reports $\chi=0.169$. However, this result erroneously integrated the differential free energy with respect to the morphing parameter λ from 0.05 to 1, rather than over the entire range of 0–1. Correcting this error gives a $\chi=0.209$ per 0.1 nm³ for PE–PEO, in good agreement with our present push–pull result of $\chi=0.218$.

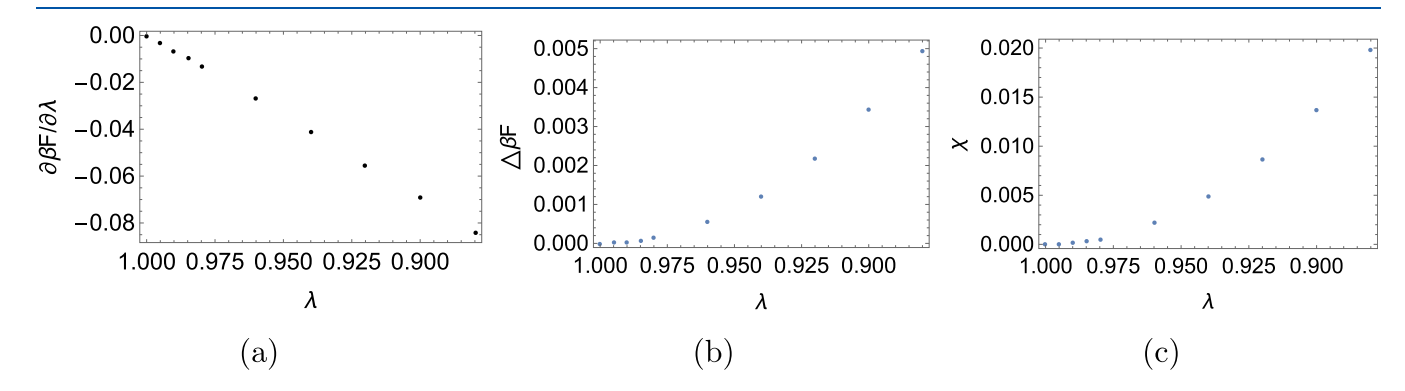


Figure 8. (a) Excess free energy integrand, (b) excess free energy, and (c) χ per bead versus morphing parameter λ , for base—weak blend.

Experimental work by Almdal et al. obtains χ for PE–PEO by measuring the order–disorder transition for diblock copolymers and fitting it to mean-field theory predictions.³³ They report χ for PE–PEO at 385 and 426 K as 0.352 and 0.269, respectively,³⁰ for a reference volume of 0.126 nm³.³⁴ We extrapolate their results to 500 K with a functional form $\chi = A/T + B$, which gives $\chi = 0.1224$ for a reference volume of 0.1 nm³. Willis et al. improved the experimental predictions of Almdal et al. and others by including corrections for polydispersity and compositional asymmetry in diblock polymers.¹⁵ Their correction to the renormalized one-loop prediction of PE–PEO diblock polymer predicts a χ of 0.1432 per 0.1 nm³ volume.¹⁴ The results are comparable to our push–pull simulation result.

Evidently, our results for χ from the push–pull method are in good agreement with our earlier results using morphing, both for bead-spring chains and for chemically realistic polymers. This is reassuring since the two methods measure the thermodynamic work to mix A and B chains in very different ways. The quantitative disagreement between our results for PE–PEO and the experimental value may reflect shortcomings in the underlying atomistic potentials, which would lead to errors in the results for both simulation methods.

DISCUSSION

Dependence of χ on System Parameters. For a binary blend of a given polymer architecture, the adjustable system parameters are the temperature, pressure, chain lengths $N_{\rm A}$ and $N_{\rm B}$, and volume fraction ϕ of the two species. Indeed, χ can depend in principle on all of these parameters. In practice, χ certainly depends on T, P, and ϕ , as has been extensively reported by experimentalists. For weak monomer-scale interactions characteristic of most polymers, we can consider long enough chains such that dependence of χ on chain length is small, as experimenters routinely do—otherwise, χ would not be a very useful parameter.

Interpretation of Measured χ . Having described in detail how we measure χ , we now reflect on its physical interpretation. Fundamentally, we have measured an equilibrium linear response function: we impose sinusoidal external potentials $U_i(z)$ that act on the position of each particle of species i, and thus couple linearly to the concentrations $\phi_i(z)$ (see eq 4); we measure the concentrations, which develop sinusoidal perturbations in response to the potentials. The induced concentration profile $\phi_i(z)$ minimizes the free energy, which can be regarded at harmonic order as the sum of the free energy cost of concentration perturbations in the absence of any potential, plus the linear couplings to the external potentials.

Effectively, we have measured the thermodynamic work required to construct the sinusoidal concentration profile. The χ parameter so determined can be understood as the quadratic term in the expansion of the free energy itself in powers of the concentration. As long as we are careful to simulate far from the critical region, and limit the strength of the external potentials so that the response is linear, a harmonic expansion of the free energy is valid.

Practically speaking, we stay away from the critical region to avoid needing (1) a larger system to represent a longer correlation length, (2) a longer equilibration time because of critical slowing down, and (3) a more sophisticated theory for analysis. More generally, renormalized one-loop theory accounts for long-wavelength fluctuations, which contribute

increasingly near the critical point. Fortunately, the critical region is relatively narrow for weakly interacting polymer blends, because for large N, the number of neighboring chains for any given chain scales as $N^{1/2}$, which tends toward meanfield behavior since each chain interacts with many others.³⁵

From our results, we know we are not in the critical region because the measured behavior of $U(\phi)$ is linear (see Figure 7). If we were approaching the critical point, $U(\phi)$ would become nonlinear, ultimately scaling as $U \propto \phi^{\delta}$ (with $\delta = 3$ in mean-field theory, and $\delta \approx 4.789$ for the 3d Ising model appropriate to the binary blend critical point). ^{36,37}

Linear Response versus Fluctuations. The χ parameter can also be determined by imitating experimentalists, who measure the structure factor S(q), which reports the variance of concentration fluctuations at wavenumber q. From S(q), χ can be determined by fitting the results to the random phase approximation (RPA). The linear response and fluctuation approaches to measuring a response function are related by the static limit of the fluctuation-dissipation theorem.

But the response function method has certain practical advantages over its fluctuation counterpart. Because the spatially varying potential is one-dimensional and time-invariant, the concentration response can be averaged both with respect to time and transverse spatial dimensions. If the potential is taken to be a cosine, the linear concentration response will likewise be a cosine, which enables Fourier filtering to remove fluctuations at other wavenumbers, for a greatly improved signal-to-noise ratio.

Both methods are subject to statistical error: both the induced concentration profile and the structure factor are time-averaged quantities and are affected by thermal fluctuations of the concentration. The question arises: how do the statistical errors for χ determined by the two methods scale with system size and simulation time, and is there any reason to prefer one method over the other? Naively, one might expect based on the fluctuation-dissipation relation that the two methods would be comparable in their efficiency, with comparable statistical errors for the same computational resources. In Appendix, we analyze this question in detail and present a scaling description for the statistical error of both approaches.

It turns out that *if* the limit of linear response corresponded to induced concentration profiles with amplitudes comparable to thermal fluctuations, the two methods would indeed be comparably efficient. Actually, linear response extends much farther; nonlinear terms act to limit swings in the concentration ϕ only near saturation i.e., (ϕ approaching zero or unity). In Figure 6d-f, plots of external potential Uversus concentration ϕ are evidently linear, corresponding to a pure cosine $\phi(z)$ in response to the cosine potential U(z). For stronger potentials than we have employed, U versus ϕ becomes steep at the ends, as $\phi(z)$ approaches the limits of its range. Because of the wide range of linear response, we can induce concentration profiles that are much stronger than thermal fluctuations, which dramatically improves the signalto-noise ratio of χ from linear response compared to χ from S(q) (see Appendix for details).

CONCLUSIONS

In this paper, we extend the push—pull method developed for small molecules to polymers. The method applies spatially varying external potential on each molecule of a given species in a blend to induce a spatial variation in the concentration. By comparing the measured relation between the applied potential

and the resulting concentration to predictions of model free energies, interaction parameters can be determined.

For polymers, square-gradient terms in the free energy density contribute significantly to the local chemical potential, tending to suppress spatially rapid concentration variations. For sufficiently large simulations, the effect of square-gradient terms can be made small. But chain entropy of mixing effects scale as 1/N, while square-gradient terms scale as a^2/L^2 , where L is the system dimension and a is a microscopic length of order the monomer size. So gradient terms are only small compared to the entropy of mixing when $L^2 \gg Na^2$. But in polymer simulations of manageable size, the simulation box dimension is often not many times larger than the mean-square end-to-end distance of the chains.

Hence, in this work, we introduce methods to measure the square-gradient coefficient a in simulations, by performing push—pull simulations on ideal mixtures. For pure melts, we can divide the chains into two groups, and pull with equal and opposite potentials on groups 1 and 2, and fit the concentration response to the prediction of ideal solution theory plus square-gradient terms. For A-B blends, we can divide both A and B chains into two groups and again pull equally and oppositely on 1 and 2, effectively performing push—pull simulations on two ideal mixtures at the same time. We use this approach to measure the square-gradient coefficient a for both bead-spring chains and chemically realistic PE and PEO oligomers. As expected on physical grounds, we find that a is a microscopic length scale, depending mainly on the persistence length of the chains.

With square-gradient coefficients available, we apply the push—pull method to compute χ for three polymer mixtures: (1) flexible bead-spring chains in which one species has weaker nonbonded interactions ("base"-"weak" blends); (2) bead-spring chains in which one species is stiffer ("base"-"stiff" blends); and (3) chemically realistic blends of PE and PEO oligomers (each consisting of 30 main-chain atoms). For each of these three systems, χ has been measured in simulations using a previously developed, more cumbersome, and more limited "morphing" method; we validate the push—pull approach by comparing to these previous results, as well as to the experimental value of χ for PE—PEO. In all cases, our present results using the new push—pull method are in good agreement with previous values.

The push–pull method has advantages over previously developed methods for measuring χ in simulations, developed by our group and by others:^{21–25}

- 1. Unlike morphing and mutual ghosting, the push—pull method requires only a single simulation, not an entire series of simulations to which some thermodynamic integration is applied.
- Unlike morphing, the push—pull method does not require that the chains under study be structurally similar so that one species can somehow be transformed into another.
- Unlike Kirkwood-Buff, very large simulations are not required to ensure good statistics and good convergence of thermodynamic integrals of pair correlation functions.

We conclude that the polymer push—pull method is versatile and widely applicable for calculating the mixing free energy between polymer mixtures with differing chemical composition and architecture; future work will leverage this versatility.

APPENDIX

Any linear response measurement in a fluctuating system at equilibrium can be made in two ways: (1) apply a small external field linearly coupled to the degree of freedom of interest and measure the average response, or (2) observe the fluctuations in the degree of freedom of interest and determine the response function from the fluctuation-dissipation theorem. This holds true for static as well as dynamic response functions.

To measure χ in simulations, we can likewise proceed in two ways. In the present work, we apply an external potential linearly coupled to the degree of freedom of interest (namely, a cosine potential coupled to the particle concentrations); measure the average concentration response; and determine χ by comparison to linear response theory. Alternatively, we can imitate experimentalists and observe the thermal fluctuations of the concentration without any external potential; measure the average structure factor S(q); and determine χ by fitting to the RPA (random phase approximation).

Each procedure is subject to statistical error. In the first method, the induced concentration profile fluctuates in time because of thermal fluctuations in the concentration. In the second method, the structure factor S(q) itself is a time-averaged quantity and likewise subject to error arising from thermal fluctuations. The question arises: for each method, how do the statistical errors scale with system size and run time? With a limited amount of computer time, which approach delivers a value for χ with smaller error?

A natural guess is that the two methods should be statistically comparable, with errors that scale in the same way; intuitively, since the fluctuation-dissipation theorem implies the two approaches are equivalent, neither should provide an advantage over the other. (Even so, there may be practical reasons to prefer one method over the other.) Since the two methods are quite different, investigating this guess requires a scaling argument for each, which we now provide. (In the following, we assume that we are far from the critical point in our simulations; otherwise, we will be plagued with slow equilibration from critical slowing down of the concentration order parameter.)

We write the concentration $\phi(r)$ as the sum of Fourier modes ϕ_q

$$\phi(r) = (1/V) \sum_{q} \phi_{q} e^{iq \cdot r}$$
(7)

In terms of the Fourier modes, the spatial integral $\int dr \phi^2(r)$ becomes $(1/V)\sum_q |\phi_q|^2$, and at harmonic order, the free energy becomes

$$\beta F = (1/V) \sum_{q} ((\chi_c - \chi) + a^2 q^2) |\phi_q|^2$$
(8)

where $\chi_c = 2/N$ is the critical value of χ . (Here and throughout, we are careless with factors of 2, which are not necessary for scaling arguments).

The Fourier modes ϕ_q are therefore Gaussian random variables with zero mean, and variance scaling as

$$\langle |\phi_q|^2 \rangle \sim \frac{V}{1/N + a^2 q^2} \tag{9}$$

In writing the above, we assume we are far from the critical point so that $\chi_c - \chi$ scales as 1/N.

In the fluctuation approach, we measure the structure factor S(q), which is the variance of each Fourier mode of concentration fluctuations ϕ_{ql} , $S(q) \sim \langle |\phi_q|^2 \rangle$. We determine χ by fitting $S^{-1}(q)$ to $A+Bq^2$; the coefficient A is $\chi_c-\chi$. To estimate the statistical error in χ by this method, we must estimate the error in the measured variance of the Fourier modes.

The variance of the variance of a Gaussian random variable scales as the variance squared. (This can be shown by explicit computation from the Gaussian distribution, or argued by dimensional analysis, since the distribution is characterized by a single parameter, its standard deviation σ .) Thus, the meansquare error in the variance of a Gaussian random variable for which we have M independent measurements scales as σ^4/M .

Because we determine χ from the reciprocal of S(q), we note that the error for the reciprocal 1/X of a quantity X scales as

$$\langle \Delta X^2 \rangle / X^2 \sim \langle \Delta (1/X)^2 \rangle / (1/X)^2$$
 (10)

(i.e., the relative errors scale the same way). Hence, we have

$$\langle \Delta (1/X)^2 \rangle \sim \langle \Delta X^2 \rangle / X^4$$
 (11)

which may likewise be argued by dimensional analysis.

To estimate an error bar for χ determined from S(q), we observe that the dominant contributions will come from q values for which the square-gradient term in $S^{-1}(q)$ is smaller than the constant term, i.e., for q such that 1/N is greater than a^2 q^2 , or equivalently for $qR_{\rm g} < 1$ (since Na^2 scales as $R_{\rm g}^2$). In a scaling sense, χ can be estimated from the average of these dominant terms. The number of such terms N^* is given by the volume in Fourier space $(q^*)^3 \sim 1/R_{\rm g}^3$, divided by the Fourier space volume element $dq^3 \sim 1/V$, which yields $N^* \sim V/R_{\rm g}^3$.

The number of independent measurements M_q of a given Fourier mode q scales as the ratio T/τ_q of the total run time T and the relaxation time τ_q of the mode. The relaxation time τ_q scales as $1/(Dq^2)$, where D is the diffusivity of the constituent molecules. Evidently, the slowly relaxing low-q modes have fewer independent measurements, and consequently larger square error.

Assembling these arguments, all of the N^* Fourier modes dominantly contributing to χ have square errors scaling like χ^2_c divided by M_a ; this leads to a square error for χ scaling as

$$\sigma_{\chi}^2 \sim \chi_{\rm c}^2 \frac{\langle 1/q^2 \rangle}{DT}$$
 (12)

in which the average $\langle \cdots \rangle'$ is carried out over the dominant modes, $|q| < 1/R_{\rm g}$. Evaluating the average leads finally to

$$\sigma_{\chi}^2 \sim \frac{\chi_{\rm c}^2 R_{\rm g}^2}{DT} \tag{13}$$

Now we develop an error estimate for the linear response method, which is considerably simpler. We apply an external potential linearly coupled to $\phi(r)$ to induce a sinusoidal concentration profile. The response function is S(q), which for long wavelengths $(qR_{\rm g}<1)$ scales as $1/(\chi_{\rm c}-\chi)$, and far from the critical point scales approximately as $1/\chi_{\rm c}$ (consistent with our assumptions and arguments above).

The square error in the response measurement is determined by the mean-square fluctuation of the induced Fourier mode ϕ_{q^*} , divided by the number of independent measurements M_{q^*} , where q^* is the wavenumber of the applied potential. For simplicity, we assume that q^* and $1/R_{\rm g}$ are comparable; in practice, we have q^* $R_{\rm g}$ < 1 but not \ll 1,

because we want to minimize the effects of square-gradient terms while keeping the total system size manageably small. The mean-square mode amplitude $\sigma_{q^*}^2$ scales as V/χ_c , and the number of independent measurements M_{q^*} scales as $T/(R_g^2/D)$. This leads to a square error estimate for the mode amplitude scaling as

$$\sigma_{q^*}^2 \sim \frac{VR_g^2}{\chi_c DT} \tag{14}$$

The square error in our linear response measurement of χ is then determined by the relative error in our value for the induced Fourier mode

$$\frac{\sigma_{\chi}^2}{\chi^2} \sim \frac{\sigma_{q^*}^2}{\langle \phi_{q^*} \rangle^2} \tag{15}$$

Evidently, we want to apply as large an external potential as we can within the limits of linear response so that the induced $\langle \phi_{q^*} \rangle$ is as large as possible relative to the magnitude of thermal fluctuations.

Naively, we might expect that the limit of linear response for a Fourier mode ϕ_q would have an amplitude comparable to the root-mean-square thermal fluctuation, i.e., ϕ_q^2 scaling as V/χ_c . If this were the case, the square error for χ measured by linear response would scale the same as for χ measured from S(q).

Actually, the limit of linear response extends much further than the typical magnitude of thermal fluctuations. Nonlinear terms in the effective Hamiltonian only begin to act on the concentration profile when the amplitude of the cosine becomes of order unity, which corresponds to a Fourier mode of amplitude V. This means the square amplitude of the mode at the limit of linear response is larger than the naive limit by a factor $V\chi_o$ or equivalently V/N, which is the number of chains in the system. Correspondingly, the relative square error in χ measured at the limit of linear response scales as a factor of N/V smaller than the corresponding relative square error in χ determined from S(q).

In summary, the wide range of linear response allows us to induce a perturbation of the concentration with an amplitude much larger than typical fluctuations, with corresponding improvements in the signal-to-noise ratio. We verify that our pulling simulations are within linear response because plots of external potential U versus concentration ϕ are in fact linear. When nonlinear terms begin to contribute, the graph of $U(\phi)$ begins to saturate, becoming steeper on the ends as ϕ approaches the limits of its range.

We speculate without proof that linear response measurements in simulation may be preferable to fluctuation measurements more generally because the limits of linear response may for various reasons exceed the range of typical fluctuations but will likely never be smaller than typical fluctuations.

AUTHOR INFORMATION

Corresponding Author

Scott T. Milner — Department of Chemical Engineering, The Pennsylvania State University, University Park, Pennsylvania 16802, United States; Department of Materials Science and Engineering, The Pennsylvania State University, University Park, Pennsylvania 16802, United States; orcid.org/0000-0002-9774-3307; Email: stm9@psu.edu

Authors

Puja Agarwala — Department of Chemical Engineering, The Pennsylvania State University, University Park, Pennsylvania 16802, United States; orcid.org/0000-0003-3561-6633

Enrique D. Gomez — Department of Chemical Engineering, The Pennsylvania State University, University Park, Pennsylvania 16802, United States; Department of Materials Science and Engineering, The Pennsylvania State University, University Park, Pennsylvania 16802, United States; Materials Research Institute, The Pennsylvania State University, University Park, Pennsylvania 16802, United States; Occid.org/0000-0001-8942-4480

Complete contact information is available at: https://pubs.acs.org/10.1021/acs.macromol.3c00793

Notes

The authors declare no competing financial interest.

ACKNOWLEDGMENTS

The authors acknowledge financial support from the National Science Foundation (DMREF-1921854) and the Office of Naval Research (N00014-19-1-2453).

REFERENCES

- (1) Hay, A. S. Polymerization by oxidative coupling: Discovery and commercialization of PPO and Noryl resins. *J. Polym. Sci., Part A: Polym. Chem.* **1998**, *36*, 505–517.
- (2) Jang, B. Z.; Uhlmann, D. R.; Sande, J. V. Rubber-toughening in polypropylene. J. Appl. Polym. Sci. 1985, 30, 2485–2504.
- (3) Vandewal, K.; Himmelberger, S.; Salleo, A. Structural factors that affect the performance of organic bulk heterojunction solar cells. *Macromolecules* **2013**, *46*, 6379–6387.
- (4) Wang, T.; Kupgan, G.; Brédas, J.-L. Organic photovoltaics: Relating chemical structure, local morphology, and electronic properties. *Trends Chem.* **2020**, *2*, 535–554.
- (5) Agarwala, P.; Gomez, E. D.; Milner, S. T. Fast, Faithful Simulations of Donor-Acceptor Interface Morphology. *J. Chem. Theory Comput.* **2022**, *18*, 6932–6939.
- (6) Jankowski, E.; Marsh, H. S.; Jayaraman, A. Computationally linking molecular features of conjugated polymers and fullerene derivatives to bulk heterojunction morphology. *Macromolecules* **2013**, 46, 5775–5785.
- (7) Cardinaels, R.; Moldenaers, P. Morphology development in immiscible polymer blends. In *Polymer Morphology: Priciples, Characterization and Properties*; Guo, Q., Ed.; John Wiley & Sons, Inc., 2016; pp 348–373.
- (8) Flory, P. J. Thermodynamics of high polymer solutions. *J. Chem. Phys.* **1942**, *10*, 51–61.
- (9) Huggins, M. L. Thermodynamic properties of solutions of long-chain compounds. *Ann. N.Y. Acad. Sci.* **1942**, 43, 1–32.
- (10) Fredrickson, G. H.; Liu, A. J.; Bates, F. S. Entropic corrections to the Flory-Huggins theory of polymer blends: Architectural and conformational effects. *Macromolecules* **1994**, *27*, 2503–2511.
- (11) Eitouni, H. B.; Balsara, N. P. Physical Properties of Polymers Handbook; Springer, 2007; pp 339–356.
- (12) Fredrickson, G. H.; Helfand, E. Fluctuation effects in the theory of microphase separation in block copolymers. *J. Chem. Phys.* **1987**, 87, 697–705.
- (13) Qin, J.; Morse, D. C. Fluctuations in symmetric diblock copolymers: Testing theories old and new. *Phys. Rev. Lett.* **2012**, *108*, No. 238301.
- (14) Grzywacz, P.; Qin, J.; Morse, D. C. Renormalization of the one-loop theory of fluctuations in polymer blends and diblock copolymer melts. *Phys. Rev. E* **2007**, *76*, No. 061802.

- (15) Willis, J. D.; Beardsley, T. M.; Matsen, M. W. Simple and accurate calibration of the Flory–Huggins interaction parameter. *Macromolecules* **2020**, *53*, 9973–9982.
- (16) Chremos, A.; Nikoubashman, A.; Panagiotopoulos, A. Z. Flory-Huggins parameter χ , from binary mixtures of Lennard-Jones particles to block copolymer melts. *J. Chem. Phys.* **2014**, *140*, No. 054909.
- (17) Panagiotopoulos, A. Z. Direct determination of phase coexistence properties of fluids by Monte Carlo simulation in a new ensemble. *Mol. Phys.* **1987**, *61*, 813–826.
- (18) Panagiotopoulos, A. Z.; Quirke, N.; Stapleton, M.; Tildesley, D. Phase equilibria by simulation in the Gibbs ensemble: alternative derivation, generalization and application to mixture and membrane equilibria. *Mol. Phys.* **1988**, *63*, 527–545.
- (19) Chen, Q. P.; Chu, J. D.; DeJaco, R. F.; Lodge, T. P.; Siepmann, J. I. Molecular simulation of olefin oligomer blend phase behavior. *Macromolecules* **2016**, *49*, 3975–3985.
- (20) Mavrantzas, V. G. Using Monte Carlo to simulate complex polymer systems: recent progress and outlook. *Front. Phys.* **2021**, *9*, No. 661367.
- (21) Venetsanos, F.; Anogiannakis, S. D.; Theodorou, D. N. Mixing Thermodynamics and Flory—Huggins Interaction Parameter of Polyethylene Oxide/Polyethylene Oligomeric Blends from Kirkwood—Buff Theory and Molecular Simulations. *Macromolecules* **2022**, *55*, 4852—4862.
- (22) Kirkwood, J. G.; Buff, F. P. The statistical mechanical theory of solutions. I. J. Chem. Phys. 1951, 19, 774–777.
- (23) Kozuch, D. J.; Zhang, W.; Milner, S. T. Predicting the Flory-Huggins χ parameter for polymers with stiffness mismatch from molecular dynamics simulations. *Polymers* **2016**, *8*, 241.
- (24) Zhang, W.; Gomez, E. D.; Milner, S. T. Predicting Flory-Huggins χ from simulations. *Phys. Rev. Lett.* **2017**, *119*, No. 017801.
- (25) Shetty, S.; Gomez, E. D.; Milner, S. T. Predicting χ of Polymer Blends Using Atomistic Morphing Simulations. *Macromolecules* **2021**, 54, 10447–10455.
- (26) Shetty, S.; Agarwala, P.; Gomez, E. D.; Milner, S. T. Predicting mixing free energy using mutual ghosting. *Mol. Syst. Des. Eng.* **2022**, *7*, 1529–1537.
- (27) Li, H.; Yan, S. Surface-induced polymer crystallization and the resultant structures and morphologies. *Macromolecules* **2011**, 44, 417–428.
- (28) Zhang, W.; Gomez, E. D.; Milner, S. T. Surface-induced chain alignment of semiflexible polymers. *Macromolecules* **2016**, 49, 963–971.
- (29) Mkandawire, W. D.; Milner, S. T. Pulling simulation predicts mixing free energy for binary mixtures. *Soft Matter* **2022**, *18*, 7998–8007.
- (30) Almdal, K.; Hillmyer, M. A.; Bates, F. S. Influence of conformational asymmetry on polymer-polymer interactions: an entropic or enthalpic effect? *Macromolecules* **2002**, *35*, 7685–7691.
- (31) Eggimann, B. L.; Sunnarborg, A. J.; Stern, H. D.; Bliss, A. P.; Siepmann, J. I. An online parameter and property database for the TraPPE force field. *Mol. Simul.* **2014**, *40*, 101–105.
- (32) Rubinstein, M.; Colby, R. H. *Polymer physics*; Oxford university press: New York, 2003; Vol. 23.
- (33) Leibler, L. Theory of microphase separation in block copolymers. *Macromolecules* **1980**, 13, 1602–1617.
- (34) Hillmyer, M. A.; Bates, F. S. Synthesis and characterization of model polyalkane- poly (ethylene oxide) block copolymers. *Macromolecules* **1996**, *29*, 6994–7002.
- (35) Fredrickson, G. H. The Equilibrium Theory of Inhomogeneous Polymers; Clarendon Press, 2006.
- (36) Ma, S.-K. Modern Theory of Critical Phenomena; Benjamin/Cummings, 1976.
- (37) Amit, D. J. Field Theory, the Renormalization Group, and Critical Phenomena; World Scientific, 1984.